Contribution of Hydrogen Bonding to Protein Stability Estimated from Isotope Effects †

ARTICLE *in* BIOCHEMISTRY · MARCH 2002

Impact Factor: 3.02 · DOI: 10.1021/bi011307t · Source: PubMed

4 AUTHORS, INCLUDING:

Bryan A Krantz
University of Maryland, Baltimore
46 PUBLICATIONS **2,593** CITATIONS
SEE PROFILE

Tobin R Sosnick
University of Chicago
161 PUBLICATIONS **8,410** CITATIONS
SEE PROFILE

Contribution of Hydrogen Bonding to Protein Stability Estimated from Isotope Effects†

Zhengshuang Shi,[‡,§] Bryan A. Krantz,[§] Neville Kallenbach,[‡] and Tobin R. Sosnick*[,§,||]

Department of Chemistry, New York University, 100 Washington Place, New York, New York 10003, and Department of Biochemistry & Molecular Biology and Institute for Biophysical Dynamics, University of Chicago, Chicago, Illinois 60637

Received June 22, 2001; Revised Manuscript Received December 4, 2001

ABSTRACT: An unresolved issue in structural biology concerns the relative contribution of H bonds to protein stability. We use the small molecules 4-acetamidobenzoic acid and *N*-acetylanthranilic acid as model compounds to relate the energetic contribution from hydrogen bonds (H bonds) to the deuterium/hydrogen amide isotope effect. *N*-Acetylanthranilic acid models carbonyl−amide H bonds formed during protein folding; 4-acetamidobenzoic acid models the unfolded state in which the amide H bonds to water. NMR is used to measure shifts in the pK_a of the ionizable carboxyl group when the amides of the compounds are either protonated or deuterated. From the pK_a shift, we obtain a quantitative scale factor: $SF = \partial(\Delta G^{HB})/\partial(RT \ln \Phi)$, where ΔG^{HB} is the change in free energy of an H bond upon isotope substitution and Φ is the fractionation factor. Isotope effect data also are reported for a small globular protein, λ repressor, using the "C_m experiment". The protein's isotope effect, which reports on the shape of the energy well, is converted to H-bonding free energy by applying the scale factor. We estimate that amide-related H bonds (amide−carbonyl and amide−water) contribute favorably to protein stability by ∼30−50 kcal/mol in λ repressor, GCN4 coiled coil, and cytochrome *c* but unfavorably by ∼6 kcal/mol in ubiquitin. The results indicate that H-bond strength varies from one protein to another and presumably at different sites within the same protein.

Since Anfinsen's original insight (*1*), the folding of a protein is generally viewed as a thermodynamically controlled reaction with a unique native structure that reflects the energetic balance of various, often competing, interactions within the protein and between the protein and the surrounding medium, water. Among the weak interactions in native proteins, hydrogen bonds (H bonds)[1] are ubiquitous and assumed to contribute to protein stability. However, the question of whether H bonds make a *net* favorable contribution has been debated for more than half a century (*2*−*5*). It is also unresolved whether H bonds contribute the same amount in different proteins or in different environments within the same protein.

In part, the controversy reflects the lack of a model system in which the stability of the H bond can be assessed independently of other factors. For example, in classical dimerization studies of small amide-containing molecules by Klotz and Franzen (*6*), it is unclear whether dimerization in water arises exclusively because of H bonding or other interactions (e.g., van der Waals or hydrophobic; *7*, *8*). Similarly, in studies of model helical peptides, significant changes in conformational entropy, van der Waals interactions, and surface burial accompany H-bond formation. Mutational studies in proteins often involve side-chain-to-backbone H bonds (*9*, *10*). Also, deletion of the side chain leads to an unknown penalty associated with the burial of the unsatisfied backbone partner. Additionally, the mutation can result in local conformational rearrangements or changes in hydrophobic surface burial that are hard to quantify (*9*).

Isotope effects offer a potential route to resolve the issue (*11*−*18*). In proteins, a qualitative correlation is observed between the H/D fractionation factor for labile protons, Φ, and H-bond strength. Sites involved in strong H bonds accumulate protium, while weak H bonds prefer deuterium, relative to the isotopic composition of the solvent (*13*). In studies on small molecules, a parabolic correlation is observed between Φ and the strength of an H bond (*19*).

Our present goal is to obtain quantitative energetic information on protein H bonds from isotope effect measurements. The scope of our study is limited to the weak H bonds commonly encountered in protein backbones (*11*−*13*, *15*−*17*, *20*). First, the D/H amide isotope effect (Figure 1) is measured for a helical protein, λ repressor using the "C_m experiment" (*15*, *18*). Next, we establish a quantitative connection between the isotope effect and the free energy of H bonds by measuring both the free-energy change of H bonds, $\Delta\Delta G^{HB}$, and the associated isotope effect.

† This work was supported in part by NIH grants to T.R.S. and by The Packard Foundation Interdisciplinary Science Program (T.R.S., P. Thiyagarajan, R. S. Berry, D. Lynn, S. Meredith).

* Corresponding author. Phone: (773) 834-0657. Fax: (773) 702-0439. E-mail: trsosnic@midway.uchicago.edu.

‡ New York University.

§ Department of Biochemistry and Molecular Biology, University of Chicago.

|| Institute for Biophysical Dynamics, University of Chicago.

[1] Abbreviations: 4-acet, 4-acetamidobenzoic acid; *N*-acet, *N*-acetylanthranilic acid; CD, circular dichroism; GdmCl, guanidinium chloride; Cyt *c*, cytochrome *c*; DMSO, dimethyl sulfoxide; $\Phi_{U/N}$, fractionation factor in N or U state; ΔG^{HB}, free energy of an H bond; ΔH^{HB}, strength (enthalpy) of an H bond; H bonds, hydrogen bonds; HX, hydrogen exchange; K_{fold}^{D}, K_{fold}^{H}, equilibrium constant for folding with deuterated, protonated amide; λ_{6-85}^{AA}, λ repressor (residues 6−85, G46A/G48A); SF, scale factor; Ub, ubiquitin.

10.1021/bi011307t CCC: $22.00
Published on Web 01/19/2002

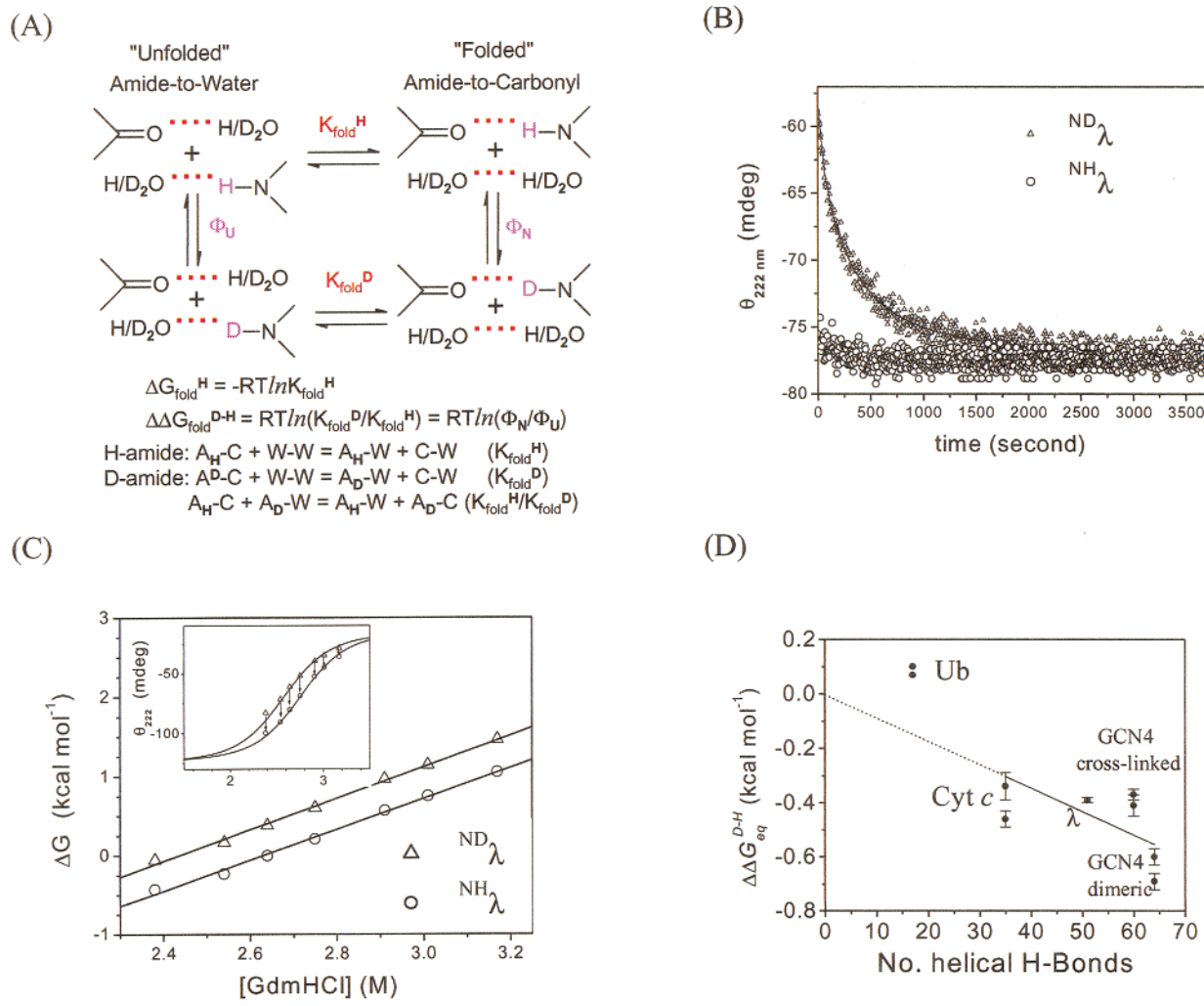

FIGURE 1: Protein backbone amide D/H isotope effects determined from the C_m experiment. (A) Thermodynamics of D/H backbone amide substitution. The isotope effect, $\Delta\Delta G_{fold}^{D-H}$, is the relative stability of protonated protein, K_{fold}^{H}, compared to the stability of deuterated protein, K_{fold}^{D}. The vertical arms are Φ values for the folded and unfolded states, respectively. The upper equations describe the relationship between $\Delta\Delta G_{fold}^{D-H}$ and the four equilibrium constants defining the thermodynamic cycle. The lower equations illustrate the relevant H bonds that influence the equilibrium of the given reactions. Notation is same as in Scheme 1; the ratio $K_{fold}^{H}/K_{fold}^{D}$ only relates to the amide−carbonyl and amide−water equilibrium, because the water−water and carbonyl−water terms cancel out. (B) Change in stability upon backbone amide D/H exchange for λ_{6-85}^{AA}. The initial and final spectroscopic values determine the equilibrium stability, K_{fold}^{D} or ΔG_{fold}^{D} (for deuterated protein) and K_{fold}^{H} or ΔG_{fold}^{H} (for protonated protein). λ_{6-85}^{AA} (10 μM) in 2.8 M GdmCl is monitored by CD at 222 nm. The deuterated protein, $^{ND}\lambda_{6-85}^{AA}$, gains stability (decreasing CD signal) when exchanged in H_2O. The control experiment, $^{NH}\lambda_{6-85}^{AA}$ diluted into H_2O solution, shows that the CD signal maintains a constant value after folding was complete. (C) Effects of isotope composition on protein stability. Values for K_{fold}^{H} and K_{fold}^{D} obtained from the C_m experiment were used to determine the denaturant dependence of free energy, ΔG_{fold}^{H} and ΔG_{fold}^{D}, under same bulk solvent condition. For each GdmCl concentration, the free energies are calculated from traces similar to that presented in (B). The mean free-energy difference between two sets of data points on the pair of lines is $\Delta\Delta G_{fold}^{D-H} = 0.39 \pm 0.01$ kcal/mol. (Inset: simulated GdmCl equilibrium melting curve for both protonated (lower) and deuterated (upper) proteins in the same H_2O solution. The arrows show the change of CD (222 nm) signal upon hydrogen exchange.) (D) Amide isotope effect versus number of helical H bonds. The slope, -9 ± 1 cal/mol, is the average isotope effect per helical H bond for the four helical proteins.

$$SF = \partial(\Delta G^{HB})/\partial(RT \ln \Phi) \quad (1)$$

This relationship is expected to be linear because the logarithm of the parabolic correlation is linear over the limited range of weak H-bond strengths investigated. Finally, we estimate the contribution to protein stability from amide-related H bonds by applying the scale factor to isotope effect data for various proteins.

MATERIALS AND METHODS

Materials. All chemicals were purchased from Sigma-Aldrich except for molecular biology reagents, which were purchased from Fisher Scientific. A protein expression vector containing the λ_{6-85}^{AA} (residues 6−85 of λ repressor, G46A/G48A) protein sequence (MSLTQEQLEDARRLKAIWEKKKNELGLSQESVADKMGMGQS AVAALFNGINALNAYNAALLAKILKVSVEEFSPSIAREIR) was created by the nested ligation of synthetic DNA oligonucleotides (Operon Technologies, Inc.) A unique *Nde*I restriction site was placed before the start of the open reading frame, and a unique *Hin*DIII site was placed after the stop codon. The λ_{6-85}^{AA} open reading frame was subcloned into pRSET B (Invitrogen) using these unique sites. λ_{6-85}^{AA} was expressed in BL21(DE3) cells in 1.5 L volumes of Luria broth using standard isopropyl-β-D-thiogalactopyranoside (IPTG) induction. Sonicated cell lysate was centrifuged at 40 000*g*, and

the supernatant pH was adjusted to 4.5 with acetic acid. After a second centrifugation at 40 000*g*, the pH 4.5 supernatant was applied to C18 HPLC and eluted by an acetonitrile gradient in 0.1% trifluoroactetic acid. The major peak was lyophilized and analyzed by gel electrophoresis. Mass spectrometry indicated the mass to be 8775 Da, which is 131 Da smaller than predicted, indicating that the N-terminal methionine was removed cotranslationally. Deuterated λ_{6-85}^{AA} is prepared by dissolving the lyophilized protein in deuterated, 7.4 M GdmCl denaturant solution.

pK_a Determination by NMR. The pH meter was calibrated using standard pH buffers at four points: 2.00, 4.00, 7.00, and 10.00 in aqueous solution at room temperature. The apparent meter reading was reported with no correction for the temperature and the effects of solvent composition. The pH probe was immersed in 90% D_2O for over 1 h before measuring the sample solutions. *N*-Acetylanthranilic acid (*N*-acet) and 4-acetamidobenzoic acid (4-acet) solutions were made at saturating concentrations in pure H_2O and pure D_2O. These stock solutions were syringe filtered, diluted 2-fold, and combined so that the final concentration of D_2O was 90%. Twenty-five 1 mL samples of *N*-acet and 4-acet solutions were prepared, and their pH was adjusted using 1 M HCl or NaOH solution in 90% D_2O. NMR spectra were collected for either compound at pHs ranging from 1.8 to 7.5 on a Varian Unity 500 MHz spectrometer. All 1D ^1H spectra with 8 k complex data points utilizing Watergate water suppression and a cycle delay of 5 s. The FIDs were transformed after weighting with a square sine function shifted by 85°. All of the experiments were performed at 20 °C in order to be consistent with the temperature at which the pHs were measured.

The apparent pK_a is determined by fitting the chemical shift values of amide or aromatic protons of model compounds at different pH values to the following equations:

$$pK_a = pH - \log([B^-]/[HB]) \quad (2)$$

$$\delta = (\delta_{base} - \delta_{acid})10^{(pH-pK_a)}/(10^{(pH-pK_a)} + 1) + \delta_{acid} \quad (3)$$

where the observed δ is the chemical shift of the amide or aromatic proton at different pH values and δ_{base} and δ_{acid} are the corresponding chemical shift values of the conjugate base (B^-) and acid (HB) forms, respectively.

D/H Amide Isotope Effect Measurement of λ_{6-85}^{AA}. The process of amide hydrogen exchange, reflected as a change in protein equilibrium stability, was monitored by circular dichroism (CD) spectroscopy at 222 ± 2 nm using a Jasco J-715 spectropolarimeter. Measurements were made for seven different GdmCl concentrations near the protein's melting midpoint, or C_m, in 20 mM sodium acetate (pH 4.5) at 10 °C. A 100-fold concentrated protein stock solution (1 mM) was diluted into a 1 cm path length cuvette containing 1.4 mL of each of the protonated GdmCl solutions. The initial signal value was used to calculate K_{fold}^D, the equilibrium constant for deuterated protein in 99% H_2O. After hydrogen exchange was complete (no further change in signal after more than 1 h; Figure 1B), the final CD signal value was used to determine K_{fold}^H, the equilibrium constant for protonated protein under the same 99% H_2O. Native and denatured baselines were measured by GdmCl equilibrium denaturation on a protonated λ_{6-85}^{AA} sample to determine the equilibrium constants from the initial and final CD signals. A standard free-energy relationship determined the isotope effect.

$$\Delta\Delta G^{D-H} = RT \ln(K_{fold}^D/K_{fold}^H) \quad (4)$$

Derivation of the Scale Factor. The correction for the contribution of solvent-related H bonds was calculated according to the relations (see Schemes 1 and 2)

$$\Delta\Delta G_{water}^{HB} = -RT \ln K_{A3} \quad (5a)$$

$$\Delta\Delta G_{corrected}^{HB} = -RT \ln K_{A7} \quad (5b)$$

$$\log K_{A7}/\log K_{A3} = \log K_{H6}/\log K_{H3} = 3.5 \quad (5c)$$

where $\Delta\Delta G_{corrected}^{HB}$ is the free energy difference between charged and neutral H bonds after correcting for the contribution from solvent related H bonds (Scheme 1). The ratio 3.5 is obtained from a series of salicylate mono-ions in both water and DMSO (*21*). The equilibrium for reaction A7 is calculated from that of reaction A3 through the solvent correction term (Scheme 2). The isotope effect is the equilibrium constant of reaction A6, calculated from the ratio of the equilibrium constants of reactions A4 and A5. The final scale factor is calculated from $\Delta\Delta G_{corrected}^{HB}$ (Scheme 1, reaction A7), and $\Delta(RT \ln \Phi)$ (Scheme 1, reaction A6, which is the isotope effect of reaction A7).

$$\Delta\Delta G_{corrected}^{HB} = 3.5\Delta\Delta G_{water}^{HB} = 3.5RT \ln (K1/K2) \quad (6a)$$

$$= 3.5RT[\ln(K1^H/K2^H) + \ln(K1^D/K2^D)]/2$$

$$\Delta(RT \ln \Phi) = -RT \ln K_{A6} = RT \ln(K_{A5}/K_{A4}) = RT(\ln K_{A5} - \ln K_{A4}) \quad (6b)$$

$$= RT[\ln(K2^D/K1^D) - \ln(K2^H/K1^H)] = RT \ln(K1^H/K1^D)$$

Numerical calculation of the scale factor takes advantage of the result that $K2^H$ and $K2^D$ are identical, as the pK_a's of the protonated and deuterated versions of the para-substituted molecule should be and are essentially identical because the amide composition has no effect on the carboxyl pK_a.

RESULTS

Equilibrium D/H Amide Isotope Effect Measurement for λ_{6-85}^{AA}. The D/H amide isotope effect in a protein is measured using the C_m experiment. The equilibrium between the native and denatured states for the protonated and deuterated proteins, K_{fold}^H and K_{fold}^D, are measured under the same solvent conditions. The ratio of these quantities defines the isotope effect independent of any solvent effects (Figure 1A). Upon amide deuteration, even a small change in stability can result in a measurable shift in the C_m or midpoint of the denaturation profile (inset to Figure 1C). Equivalently, the fraction of folded protein, and hence CD signal, significantly changes when the protein amides are exchanged from deuterium to protium near the C_m (Figure 1B).

We have used the change in CD signal to quantify the change in stability upon isotope exchange for a variant of the λ repressor, λ_{6-85}^{AA}. This monomeric helical protein is

Scheme 1[a]

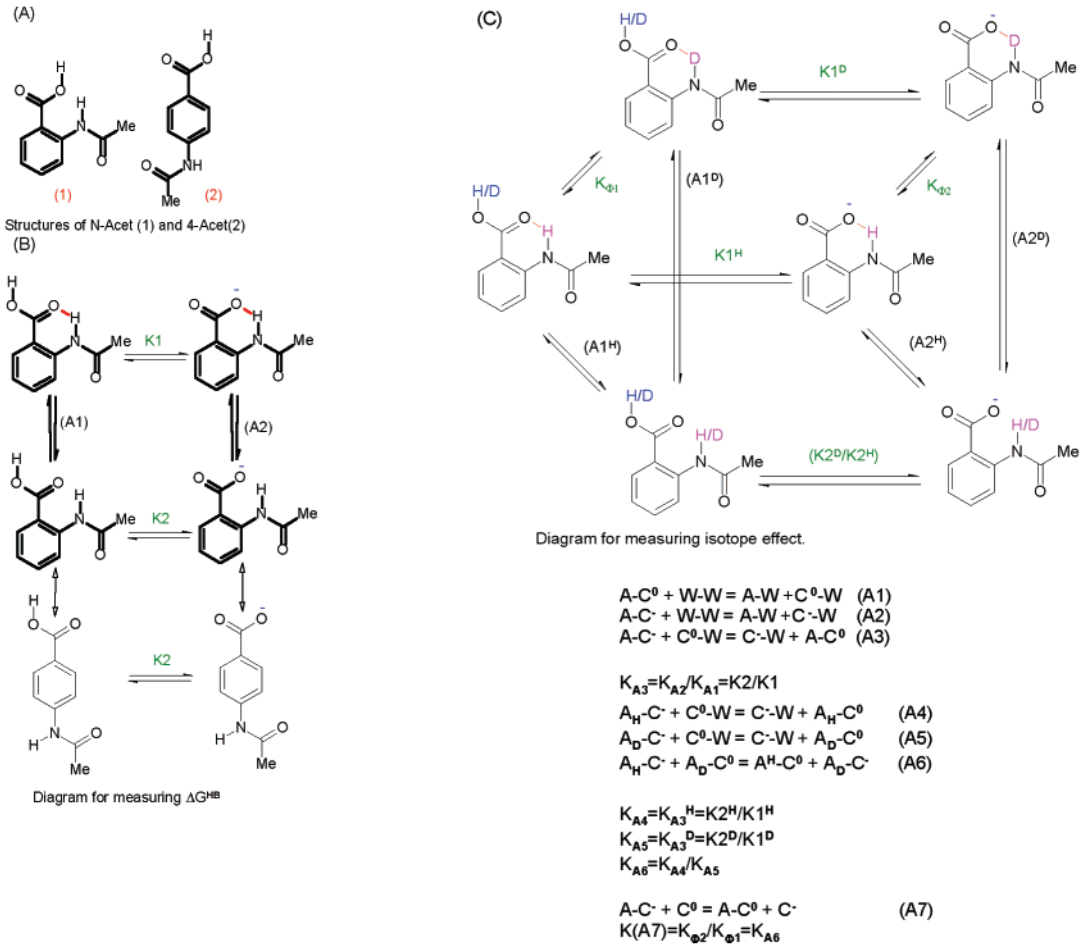

A-C⁰ + W-W = A-W + C⁰-W (A1)
A-C⁻ + W-W = A-W + C⁻-W (A2)
A-C⁻ + C⁰-W = C⁻-W + A-C⁰ (A3)

$K_{A3}=K_{A2}/K_{A1}=K2/K1$

A_H-C⁻ + C⁰-W = C⁻-W + A_H-C⁰ (A4)
A_D-C⁻ + C⁰-W = C⁻-W + A_D-C⁰ (A5)
A_H-C⁻ + A_D-C⁰ = A^H-C⁰ + A_D-C⁻ (A6)

$K_{A4}=K_{A3}{}^{H}=K2^{H}/K1^{H}$
$K_{A5}=K_{A3}{}^{D}=K2^{D}/K1^{D}$
$K_{A6}=K_{A4}/K_{A5}$

A-C⁻ + C⁰ = A-C⁰ + C⁻ (A7)
$K(A7)=K_{\Phi 2}/K_{\Phi 1}=K_{A6}$

[a] (A) Structures, (B) H bonding, and (C) isotope effects. *K*1 is the pK_a equilibrium for compound (1); *K*2 is for compound (2); and $K1^D$, $K1^H$ and $K2^D$, $K2^H$ are the corresponding equilibrium when the amide is D or H. Note that, for $K2^H$ and $K2^D$, the pK_a's of the proteated and deuterated versions of the para substituted molecules should be and are essentially identical because the amide composition has no effect on the carboxylate pK_a of the para molecule. The lower equations indicate the relevant H bonds that influence the equilibrium of the given reactions: A, amide; C^0, neutral form of carboxyl; W, water; C^-, charged form of carboxyl; A_H, proteated amide; A_D, deuterated amide; A−C^0, H bond between A and C^0, and so forth.

Scheme 2[a]

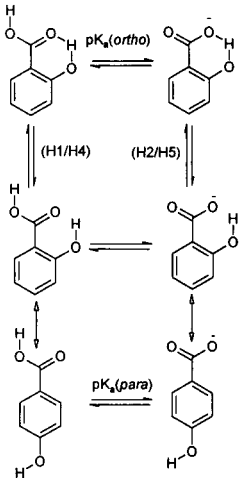

H-C⁰ + W-W = H-W + C⁰-W (H1)
H-C⁻ + W-W = H-W + C⁻-W (H2)
H-C⁻ + C⁰-W = C⁻-W + H-C⁰ (H3)
H-C⁰ + DMSO = H-DMSO + C⁰ (H4)
H-C⁻ + DMSO = H-DMSO + C⁻ (H5)
H-C⁻ + C⁰ = H-C⁰ + C⁻ (H6)

[a] H, hydroxyl; C^0, the neutral form of carboxyl; W, water; C^-, charged form of carboxyl; H−C^0, H bond in salicylic acid between H and C^0; H−C^-, H bond between H and C^-.

chosen because extensive thermodynamic and kinetic studies have previously been reported. The protein folds via a two-state mechanism on a ms−μs timescale (*22*−*24*). Experimentally, fully deuterated protein is diluted 100-fold into an appropriate concentration of GdmCl solution under conditions (pH 4.5, 10 °C) where stability (monitored by CD at 222 nm) can be determined before significant backbone amide exchange occurs (Figure 1B). Under this condition, the protein can fold in less than a second and equilibrates to the new solvent condition. Hence, the stability of deuterated protein can be obtained from the initial CD value. As the hydrogen exchange (HX) process occurs over 1 h, the equilibrium of the system shifts, and the spectroscopic signal continuously changes. After HX is complete, the stability of the now protonated protein is measured. The difference in stability before and after amide exchange defines $\Delta\Delta G_{fold}{}^{D-H}$ (Figure 1A).

To re-emphasize, we conduct our measurements near the C_m, where even a small perturbation such as isotope substitution can be detected accurately. Furthermore, we repeated this measurement at seven different GdmCl concentrations within the melting transition region. The corresponding free energies, $\Delta G_{fold}{}^{D}$ and $\Delta G_{fold}{}^{H}$, are shown in Figure 1C, from which we obtain a nearly constant value of $\Delta\Delta G_{fold}{}^{D-H} \sim 0.39 \pm 0.01$ kcal/mol.

Strategy for Scale Factor Determination. To determine the scale factor, we have chosen a system to measure the free-energy change and the associated isotope effect for H bonding. Salicylic acid has been used previously to study H bonds (*21*, *25*). In this molecule, a second six-member ring is created upon H-bond formation. Rather than utilizing salicylic acid in which the carboxyl's H bonding partner is a hydroxyl group, we use *N*-acet where the H bond is formed using an authentic amide group. For either model compound, the change in free energy of H bonds, $\Delta\Delta G^{HB}$, with the ionization state of COOH (neutral or negatively charged) can be obtained via pK_a shift measurements. Hence, the numerator of the scale factor relating ΔG^{HB} to the isotope effect is determined (eq 1).

As outlined in Scheme 1B, the stability of the amide−carboxylate H bond of *N*-acet depends on the charge state of the carboxyl group and, therefore, on the pH. Because of the H bond, the pK_a of the ortho-substituted molecule is lower than that of the para-substituted molecule, which cannot form an intramolecular H bond. This shift in the pK_a reflects the difference of the stability between neutral and charged H bonds, $\Delta\Delta G^{HB} = -RT \ln(K_{A3})$.

We now need to determine the associated isotope effect. We have designed an experiment (Scheme 1C) to measure the free-energy difference (via the shift in pK_a of an ortho compound relative to a para compound) in *N*-acet for both the protonated, $\Delta\Delta G^{H}$, and the deuterated amide, $\Delta\Delta G^{D}$. The difference between these two values, $\Delta\Delta G^{H} - \Delta\Delta G^{D}$, yields the isotope effect. This effect is the ratio of the Φ value of the amide hydrogen when bonded to the charged group relative to the Φ value of the amide H bonded to the neutral group. From this free-energy difference ($\Delta\Delta G^{H} - \Delta\Delta G^{D}$), we obtain the Φ value component of the scale factor that relates H-bond stability to the D/H isotope effect (eq 1; see Materials and Methods).

Experimental Determination of Scale Factor. To determine the scale factor, the difference in stability is assessed between the charged and the neutral intramolecular H bonds of *N*-acet in aqueous solution. The free-energy difference between the amide−carboxyl H bonds in the charged and neutral forms is obtained from the shift of the pK_a of the COOH group in *N*-acet relative to the COOH in 4-acet. The para compound is used to approximate the intrinsic pK_a of the ortho compound when the intramolecular H bond is not formed (Scheme 1B). The pK_a shift (i.e., $pK_a^{ortho} - pK_a^{para}$) is the logarithm of the equilibrium constant for the reaction A3. This reaction reflects the change in intramolecular H-bond stability upon going from uncharged (amide−carbonyl or amide−hydroxyl) to charged (amide−oxyanion) states *relative* to the change in stability for the intermolecular H bonds to water.

The pK_a values are determined by monitoring the ^{1}H NMR chemical shifts during pH titration. All pK_a measurement experiments are performed in the same (90% D_2O) composition of bulk solvent. Use of the same solvent results in the shifts being exclusively associated with changes in ionization and amide isotope composition, rather than with changes in bulk solvent, which may have secondary isotope effects due to a change in solvent properties such as hydrophobicity or dielectric constant.

Amide and aromatic peaks are used for the determination of $K1^H$ and $K1^D$, respectively (Figure 2). The equilibrium constant relevant for the protonated amide is measured directly from the change in its chemical shift upon ionization of the acid. The equilibrium for the deuterated form is monitored indirectly via the ^{1}H aromatic resonance. The aromatic resonance associated with the deuterated amide group is about 10-fold larger than that associated with the protonated resonance because of the high level of deuterium in the 90% D_2O solvent. Moreover, these resonances are sensitive to the charge state of the carboxyl group. Thus, the apparent pK_a is determined by fitting chemical shift values of the amide and the aromatic protons (Figure 3, Table 1), thereby evaluating the equilibrium constants $K1^H$ and $K1^D$, respectively (Scheme 1). The ionization constants for the states in which the amide and COOH are H bonded to solvent, $K2^D$ and $K2^H$ (Scheme 1), cannot be obtained directly because of the formation of the intramolecular H bond. The values for these equilibria are approximated using the para-substituted compound 4-acet.

From the data on the ortho and para molecules, we obtain the shift in pK_a values for both the protonated and deuterated amides and, by implication, the ratios $K2^H/K1^H$ or $K2^D/K1^D$, as shown in Scheme 1. For both isotopes, the ratio $K2/K1$ is the equilibrium constant of equation A3, obtained by subtraction of reaction A2 from reaction A1 to eliminate the contributions from both water−water and amide−water H bonds. Reaction A3 reflects either the difference in stability for the H bond of the ortho molecule in its neutral and charged forms (vertical reactions in Scheme 1B) or the ratio $K1/K2$, measured using pK_a's of molecules of ortho and para forms (horizontal reactions).

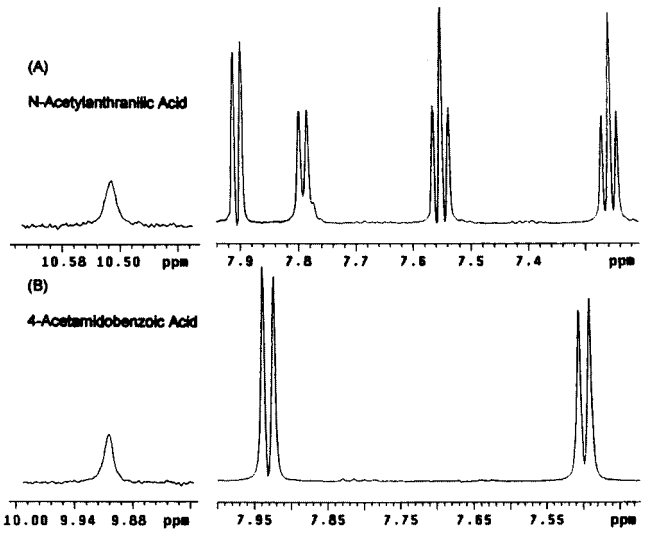

FIGURE 2: Amide (left) and aromatic regions (right) from ^{1}H spectra of (A) *N*-acet and (B) 4-acet. The vertical scales of amide peaks are enlarged 5-fold for clarity.

Table 1: pK_a Values of Model Compounds Obtained in 90% D_2O at 20 °C

equilibrium constant	pK_a ($-\log K$)
$K1^H$	3.617 ± 0.007
$K2^H$	4.330 ± 0.011[a]
$K1^D$	3.650 ± 0.007[b]
$K2^D$	4.340 ± 0.008[a,b]

[a] The values for $K2^H$ and $K2^D$ are essentially identical because the D/H amide composition has no effect on the carboxyl pK_a for the para molecule. [b] Values for deuterated equilibrium are the average of two unique aromatic resonances.

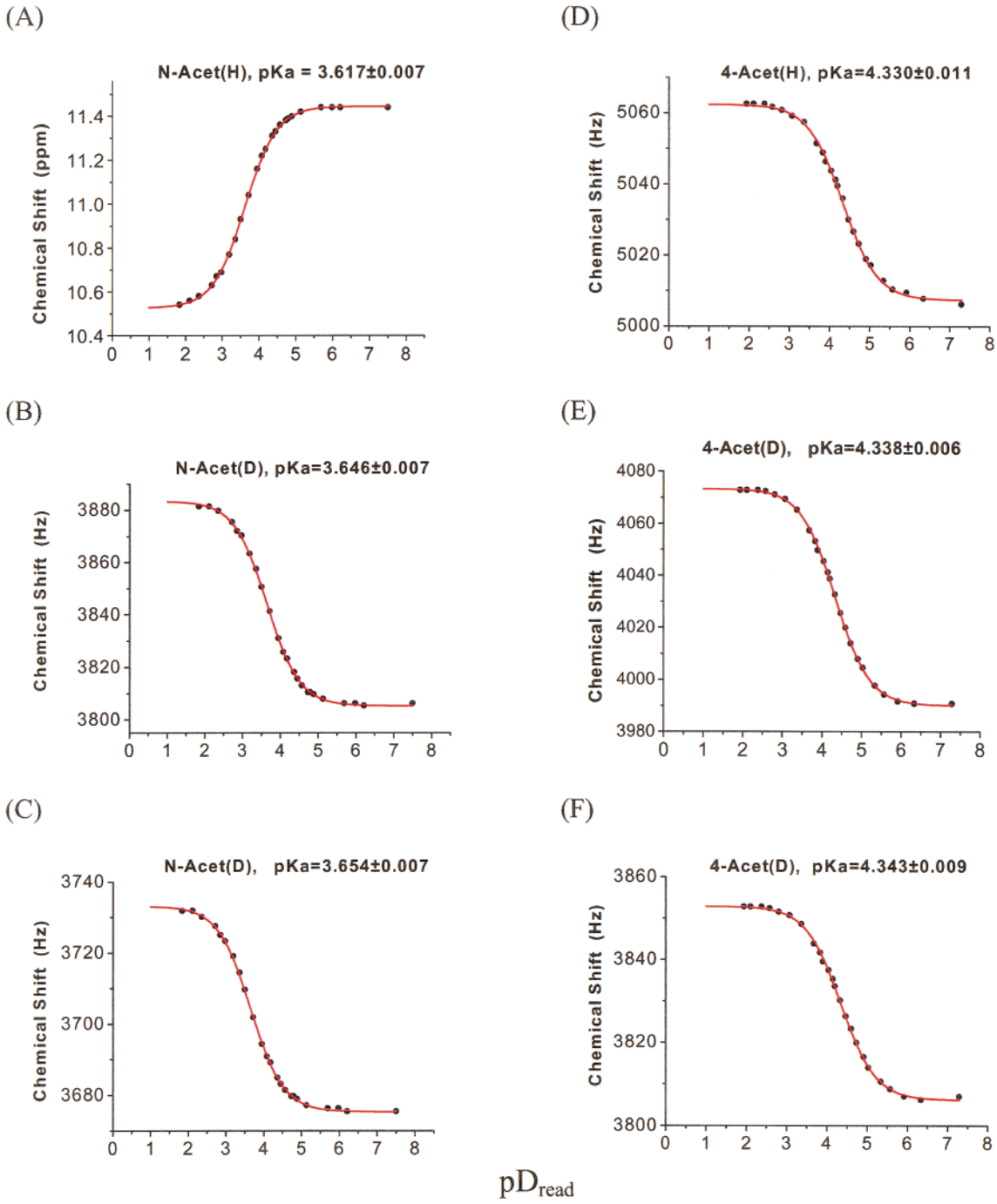

FIGURE 3: Measurement of pK_a using NMR chemical shifts. Panels A−C are pH titrations of *N*-acet. (A) The shift in amide resonance is used to obtain $K1^H$ of the protonated molecule, *N*-acet(H). (B and C) The shift in the aromatic resonances is used to obtain $K1^D$ of the deuterated molecule *N*-acet(D), done for two separate peaks. Panels D−F are pH titrations of 4-acet. (D) The shift in amide resonance is used to obtain $K2^H$ for 4-acet(H). (E and F) The shift in the aromatic resonances is used to obtain $K2^D$ for 4-acet(D).

By subtracting reaction A5 from reaction A4 (Scheme 1C), we obtain an equilibrium constant for reaction A6 where the contributions involving water cancel, because both ratios, $K2^H/K1^H$ and $K2^D/K1^D$, are derived from experiments conducted in the same solvent. The equilibrium constants for the protonated (A4) and deuterated (A5) reactions are the ratios $K2^H/K1^H$ and $K2^D/K1^D$, respectively. These ratios can be used to derive the ratio of the Φ values for the amide with its H-bonding partner being an oxyanion relative to the amide with its partner being a neutral carboxyl (Scheme 1, reactions A6 and A7).

Correction for Solvent H Bonding. As seen in eq 5a, $\Delta\Delta G_{water}^{HB} = -RT \ln K_{A3}$ is the difference in stability between the charged and the uncharged carboxyl−amide H bonds relative to the difference in stability between the charged and uncharged carboxyl−water H bonds. This quantity is influenced by solvent H bonding, as shown in reaction A3 (Scheme 1). However, the measured $\Delta(RT \ln \Phi)$, the ratio of Φ values for the amide hydrogen in the amide−oxyanion and amide−carboxyl bonds, is not directly influenced by solvent H bonding, as shown in reaction A7. To relate H-bond strength to Φ values of relevance, we must

Table 2: Amide Isotope Effects and H-Bonding Contribution to Protein Stability

proteins	$\Delta\Delta G^{D-H}$ (isotope effect) (kcal/mol)	$\Delta\Delta G^{HB}$ (from H bonds) (kcal/mol)	no. of H bonds	$\Delta\Delta G^{HB}$/H bond (kcal/mol)
$\lambda_{6-85}{}^{AA}$	-0.39 ± 0.01	-29	56	-0.52
GCN4 (cross-linked)[a]	-0.37 ± 0.02	-29	60	-0.48
	-0.41 ± 0.02			
GCN4 (dimeric)[a]	-0.60 ± 0.03	-48	64	-0.75
	-0.69 ± 0.03			
cytochrome *c*[a]	-0.34 ± 0.05	-30	51	-0.58
	-0.46 ± 0.03			
ubiquitin[1]	0.07 ± 0.01	6	45	0.1
	0.10 ± 0.02			

[a] Kinetic isotope effect measured derived from equilibrium (upper values) and kinetic (lower values) measurements in Krantz et al. (*18*).

correct $\Delta\Delta G^{HB}$ by the contributions from the solvent-related H bonds.

A study in an aprotic solvent (e.g., dimethyl sulfoxide (DMSO)) can provide an estimate of the contribution from solvent-related H bonds. Shan and Herschlag (*21*) measured the pK_a shift for a series of substituted salicylate mono-ions in water and DMSO. Their data indicate that the H bond undergoes a large apparent increase in strength upon transfer from water to DMSO. Specifically, the equilibrium constants for reactions H3 and H6 in Scheme 2 are the measured pK_a differences in water and DMSO, respectively. From reactions H3 and H6 in Scheme 2, the equilibrium constant for H6 should be larger than that for H3, even if the strength of an H bond (i.e., hydroxyl−carboxyl or hydroxyl−oxyanion) does not change in water relative to that in DMSO. For the H3 equilibrium, there are offsetting H bonds formed with water for both the charged and neutral carboxyl groups, while such a cancellation does not occur in DMSO for the H6 equilibrium.

We utilized the difference between pK_a values in water and DMSO to correct the free-energy data in water and obtained the net difference in stability between the charged and the uncharged carboxyl−amide H bonds without the influence from solvent H bonding. For the series of salicylate mono-ions, log K_{H6}(DMSO)/log K_{H3}(water) $\sim$ 3.5 (Scheme 2). Assuming that this ratio can be applied to our *N*-acet data, we can get the equilibrium constant for reaction A7 from that of A3 (Scheme 1). After correcting for the solvent, we finally obtain the scale factor SF $= 74 \pm 27$.

Application of the Scale Factor to Proteins. Given that the scale factor derived from the model compound can be applied to amide-related H bonds in proteins, we are now in a position to estimate the difference in stability between a native amide−carbonyl bond and an unfolded amide−water bond $\Delta\Delta G^{HB}$ from their isotope effects. We observed that, for $\lambda_{6-85}{}^{AA}$, the coiled coil helical protein GCN4, and cytochrome *c* (Cyt *c*), deuteration results in a destabilization by about 0.4−0.7 kcal/mol, while for the α/β protein ubiquitin (Ub), deuteration results in a mild stabilization of $\sim$0.1 kcal/mol (*18*) (Table 2). These isotope effects imply that, for $\lambda_{6-85}{}^{AA}$, GCN4, Cyt *c*, and Ub, the amide-related H bond makes a net favorable contribution of 29, 30−51, 34, and −6 kcal/mol, respectively. The results for the helical proteins imply that the average amide-related H bond is worth 0.7 ± 0.3 kcal/mol. For Ub, however, the average contribution per bond is slightly *unfavorable* by $\sim$0.1 kcal/mol. These results indicate that H bonds contribute differently in different proteins.

These experiments focus exclusively on energetic contributions from amide−carbonyl H bonds and amide−water H bonds. The water−water and carbonyl−water H bonds, the solvation of water molecules freed upon folding, and the desolvation terms from amide−water and carbonyl−water H bonds must be taken into account as well when considering whether H bonds have a net stabilizing effect in protein folding.

Error Analysis. Even with the careful measurement of isotope effects and free energy changes in the model compounds, we find a significant error in the scale factor, SF $= 74 \pm 27$. The error comes from uncertainties in the values of $\Delta(RT \ln \Phi)$ and $\Delta\Delta G^{HB}$. Because the isotope effect is intrinsically small, the largest source of statistical error comes from the determination of $\Delta(RT \ln \Phi)$. To obtain this quantity, we measured a pK_a difference of 0.033 between deuterated and protonated model compounds with an uncertainty of 0.007. Compared to the error for $\Delta(RT \ln \Phi)$, the accuracy in the determination of $\Delta\Delta G^{HB}$ is much higher. This quantity is obtained from the difference in pK_a between the ortho and para molecules, which is about 0.70 ± 0.01.

Other uncertainty is associated with the correction for solvent H bonding. This correction is on the order of 3000 in terms of K_{eq}, or log $K_{eq} \sim 3.5$. Although this correction is large in absolute value, the quoted error in the SF value is relatively insensitive to the magnitude of this solvent correction. This is because the statistical error in $\Delta(RT \ln \Phi)$ is larger than the likely uncertainty in the value of the solvent correction term. The quoted error in SF is equivalent to a range of the solvent correction from 170 to 64 500 in terms of K_{eq} (2.2 and 4.8 in terms of log K_{eq}). On the basis of measurements in both DMSO and water (*21*), we estimate the range for the solvent correction term to be $\sim$1300 to $\sim$5800. This range is much smaller than 170 to 64 500, the range reflecting the statistical uncertainty in the SF. Hence, this solvent correction term does not introduce an uncertainty that exceeds the quoted statistical error. Last, for the H/D isotope effect measurements in five proteins studied, the statistical errors are generally small (e.g., 0.39 ± 0.01 kcal/mol for $\lambda_{6-85}{}^{AA}$; Table 2).

DISCUSSION

We have introduced an alternative method to investigate H-bond strength through its relationship with the amide isotope effect (*11*−*17*). Some details of the isotope effect, however, are poorly understood (*20*, *21*, *26*−*46*) although there have been numerous attempts to uncover the relationship between fractionation factors, H-bond strength, the

geometry of the donor and acceptor, the related NMR chemical shifts, and nuclear scalar spin−spin coupling constants (*47*−*51*). In proteins, stronger H bonds energetically prefer protium to deuterium. The underlying basis of this preference is the change in zero-point vibrational energy caused by the change in mass of the bridge atom within an H bond. However, the shape of the energy well, and therefore the isotope preference of a particular H bond, may be complex. The isotope effect is governed by local factors, including the detailed geometry of the bond and the intrinsic pK_a's of donor and acceptor. These factors are reflected in the change in the effective vibrational force constant that is directly relevant to the strength of the H bond.

Fractionation factors for small molecules have been measured extensively by NMR, infrared spectroscopy, and tritium labeling in both gas and solution phases (*19*). In certain situations H bonding has been shown to produce very large isotope effects; in particular, in the case of single-well or "low-barrier" H bonds, where the H bond may be unusually strong and fractionation values decrease to around 0.5 (*20*). From studies of small molecules, a parabolic correlation is found between Φ and the strength of an H bond. Our study, however, is limited to one side of the parabola applicable to the weak H bonds commonly encountered in protein backbones (*11*−*13*, *15*−*17*, *20*).

Amide H Bond Strength in Proteins. We have applied the relationship between ΔG^{HB} and isotope effects from *N*-acet to the isotope effect data for proteins to estimate the net stabilization of H bonds. To do so, we assume that the fractionation factor, which reports on the shape of the energy well, is correlated with the stability of an H bond. This assumption is based upon the observation that, in proteins, a qualitative correlation is observed between fractionation factors and the stability of H bonds, with sites involved in strong H bonds accumulating protium while weak H bonds prefer deuterium (*13*, *19*).

We also assume that the scale factor derived from the model compounds is linear and applicable to amide-related H bonds in proteins, even though each bond may obey its own precise relationship. By using the C_m experiment, we have obtained the D/H isotope effect of $\lambda_{6-85}{}^{AA}$ and find that the deuterated protein is destablized by 0.39 kcal/mol relative to the protonated version.

The cumulative data for these helical proteins, $\lambda_{6-85}{}^{AA}$, GCN4, and Cyt *c* (Figure 1D), indicate that the average isotope effect per helical H bond is -9 ± 1 cal/mol. Multiplication of this value by the SF indicates that the average amide-related H bond in a helix contributes about 0.7 ± 0.3 kcal/mol to protein stability. The near-zero or slightly unfavorable net value for Ub, which contains almost an equal number of sheet and helical H bonds, could imply that bonds in β sheets are similar in magnitude but opposite in sign to those in helices. Alternatively in Ub, there may be some buried amides that fail to form H bonds at all (e.g., Ile3) and consequently have an unusually high Φ_N value that largely offsets the favorable contributions of bonds in both sheets and helices. Other studies on seven β or α/β proteins indicate that the average isotope effect in sheets is nearly zero (Krantz and Sosnick, unpublished data), indicating that the average amide H bond in sheets is equivalent in energy to the amide−water H bond.

The geometries of H bonds are variable, especially the angles between the N−H and O═C groups in helices and parallel and antiparallel β-sheets. Hence, it may not be surprising to find that H bonds contribute differently in different proteins and in different secondary structures and environments within the same protein. Helical H bonds often have a nearly optimal bonding geometry, whereas H bonds in sheets often are suboptimal, both intrinsically as for parallel sheets as well as because of the twisting of the stands (*52*). The intrinsic pK_a for each amide and carbonyl group can differ significantly, even for the same residue in a different sequence (*53*). This difference in pK_a should also affect the stability of each H bond.

Further, we stress that the conclusion that backbone H-bond formation is net stabilizing depends critically upon the relative stability of water−water bonds that are recovered and the carbonyl−water bonds that are lost during the refolding reaction. For example, if water−water H bonds ($\Delta H \sim 6.7$ kcal/mol per H bond (*54*)) are stronger than water−carbonyl H bonds, the formation of H bonds in Ub could still be net stabilizing, even though the amide-related bonds are slightly net destabilizing. Available thermodynamic data, excess molar enthalpies for the binary system of acetone and water, suggest that water−water H bonds are probably (enthalpically) stronger than water−acetone H bonds (*55*). Hence, we propose that the formation of water−water H bonds provides a significant contribution to protein stability.

Because only the amide composition is changed in the isotope effect measurement, the values we derive relate to the amide-related H bonds and do not contain significant contributions from other interactions that accompany H bond formation during folding. In our C_m experiment, the N ↔ U equilibrium when the amides are deuterated is compared to that when the amides are protonated. Other factors, such as polar and nonpolar surface burial, backbone desolvation, and conformational entropy, contribute equally to both the deuterated and protonated equilibria. Hence, these other factors cancel in $\Delta\Delta G^{D-H} = \Delta G^{D} - \Delta G^{H}$, leaving only the difference between the deuterated and protonated amide-related H bonds.

In our analysis, we attempt to identify the energetic contribution from individual H bonds to protein's stability. Although free energies are often decomposed in biophysical analyses such as helix-coil theory, Mark and van Gunsteren (*56*) correctly noted that the separation of a Hamiltonian, which is composed of two terms, can only be done when the interactions operate on different coordinates. Hence, decomposition of the free energy into contributions of individual interactions within a cooperative system is an extremely difficult process. In general, it is not possible to identify a free energy associated with an individual interaction, such as an H bond, because one cannot conduct an experiment that exclusively perturbs this component.

A large amount of the literature, however, rests on the assumption that some differential effect—spectroscopic, calorimetric, or mutational—can be attributed to a particular interaction despite a lack of complete rigor. Furthermore, Sharp and co-workers (*57*, *58*) extended the analysis of Mark and van Gunsteren and concluded that, in practical terms, it is often possible to separate out different free-energy contributions.

In our case, an assessment of the net energetic contribution from amide-related H bonds is of fundamental interest and importance. The energetic contribution we estimate is for the component that is perturbed by isotopic substitution. This contribution probably will be dominated by H bonds and not include other terms (e.g., configurational entropy, desolvation, van der Waals), because the SF is derived from a measurement in a small molecule model where the difference in stability of two conformations is largely due to changes in the H bond strength and not the other quantities. Likewise, the change in protein stability upon addition of a neutron to each amide hydrogen largely alters just the H bond interaction. Our strategy is based upon the assumption that these two quantities can be combined to estimate the net contribution of H bonds in a native protein independent of the other components. This contribution is apportioned to individual H bonds, because a change in strength of an H bond at one amide site is unlikely to directly influence the strength of an H bond at another amide site (*18*). In this situation, different H bonds should act independently and be separable.

Isotope effects and pK_a's reflect equilibrium populations. Hence, the measured values for H bonding reflect free-energy differences. Because the isotope measurement does not involve a change in protein conformation, the predominant component may be enthalpic. What we term here the "strength of an H bond" probably refers more to differences in enthalpy rather than free energy as it originates from the shape difference of the potential energy between H and D bonds. Hence, $\Delta\Delta G$ maybe be nearly equivalent to $\Delta\Delta H$ in this case

$$\mathrm{SF} = \partial(\Delta G^{\mathrm{HB}})/\partial(RT \ln \Phi) \approx \Delta\Delta H^{\mathrm{HB}}/\Delta(RT \ln \Phi) \quad (7)$$

although we cannot conclude this from our data. However, amide−water H bonds are involved in the equilibrium, and presumably water entropy plays a role as well.

Helix Formation and Comparisons to Other Studies. The observed contribution from amide-related H bonds in a helix, 0.7 ± 0.3 kcal/mol per residue, is insufficient to account for helix formation in proteins. The change in backbone conformational entropy for an alanine upon helix formation is estimated to be ~1.2 kcal/mol (*59*). Given that the Zimm−Bragg equilibrium constant, s_{alanine}, is ~1.7 (*60*), or $\Delta G \sim$ 0.3 kcal/mol, other factors, both favorable and unfavorable, must combine to contribute the remaining 0.8 kcal/mol in free energy required for helix formation. Favorable contributions may include water−water H bonds, van der Waals interactions, and hydrophobic effects as well as solvent−helix interactions; unfavorable interactions include carbonyl−water H bond and desolvation (*61*). Scholtz et al. (*62*) determined $\Delta H = 1.0-1.3$ kcal/mol per residue for the α-helix-to-coil transition of alanine peptides in water, which is greater than our value of ~0.7 kcal/mol for amide-related helical H bonds. We believe their value includes these contributions just mentioned.

An exact comparison is difficult to make between the present study and previous estimates of the net strength of an H bond. The stability derived from the isotope effect measurement reflects the energetic contribution exclusively from the amide−carbonyl and amide−water H bonds, with none of the additional contributions that are normally included in other measurements such as polar desolvation. For example, Pace and co-workers estimated $\Delta G \sim -1$ to -2 kcal/mol per H bond from mutational studies, which includes both the loss of water−carbonyl and the gain in water−water H bonds, in addition to the transfer of the H bond from solution to the interior of the protein (*9*, *10*). Similarly, Ross and Rekharsky (*63*) determined the equilibrium constants for a series of small organic molecules binding to cyclodextrins, concluding that, at room temperature, one H bond contributes −0.6 kcal/mol to the stability of the complex. A number of theoretical studies arrive at the opposite conclusion (*5*, *64*, *65*), arguing that the significant penalty associated with desolvation of the polar groups offsets any gain in H bond stability.

CONCLUSION

We have established a relationship between H bond free energy and amide isotope effects. By applying a scale factor connecting these two quantities, we can estimate the energetic contribution of amide-related H bonds through the measurement of its isotope effect. Inherent to fractionation measurements, this estimate only pertains to the energetic contribution from amide−carbonyl and amide−water H bonds, without significant contributions from other interactions that accompany H bond formation during folding.

On the basis of the difference in the isotope effect for native and denatured states, H bond contributions appear to vary among different proteins and even among different sites within the same protein. The contribution from amide-related H bonds is favorable by ~30−50 kcal/mol for the helical proteins $\lambda_{6-85}{}^{\mathrm{AA}}$, GCN4 coiled coil, and Cyt *c*, but the contribution is unfavorable by 6 kcal/mol for the α/β protein Ub. A backbone H bond at a helical position is about 0.7 kcal/mol more stable than the corresponding amide−water H bond. In contrast, an H bond within a β sheet may provide no stability or even may be less stable than the corresponding amide−water H bond. Hence, it seems a helical H bond provides at least 0.7 kcal/mol more stability to a protein than does a sheet H bond.

These results indicate that helical H bonds can provide a significant contribution to protein stability, provided that water−water H bonds are stronger than carbonyl−water bonds. The net contribution of H bonds to the overall stability of a protein depends also on terms such as solvation and desolvation, which we have not measured. Nevertheless, calibration of the scale factor relating H bond stability to isotope effects, in conjunction with site-resolved measurements, provides a method to estimate energetic contribution from individual H bonds in a protein, a valuable quantity for studies of protein stability and function.

ACKNOWLEDGMENT

We thank J. Piccirilli, A. Kentsis, D. Herschlag, K. Sharp, B. Honig, S. W. Englander, A. Fernández, and R. L. Baldwin for enlightening discussions and comments on the manuscript.

REFERENCES

1. Anfinsen, C. B. (1956) *J. Biol. Chem. 221*, 405−412.
2. Pauling, L., Corey, R. B., and Branson, H. R. (1951) *Proc. Natl. Acad. Sci. U.S.A. 37*, 235−240.
3. Pace, C. N. (1995) *Methods Enzymol. 259*, 538−554.

4. BenTal, N., Sitkoff, D., Topol, I. A., Yang, A. S., Burt, S. K., and Honig, B. (1997) *J. Phys. Chem. B 101*, 450−457.
5. Dill, K. A. (1990) *Biochemistry 29*, 7133−7155.
6. Klotz, I. M., and Fransen, J. S. (1962) *J. Am. Chem. Soc. 84*, 3461.
7. Roseman, M. A. (1988) *J. Mol. Biol. 201*, 621−623.
8. Jorgensen, W. (1989) *J. Am. Chem. Soc. 111*, 3770−3771.
9. Myers, J. K., and Pace, C. N. (1996) *Biophys. J. 71*, 2033−2039.
10. Pace, C. N., Shirley, B. A., McNutt, M., and Gajiwala, K. (1996) *FASEB J. 10*, 75−83.
11. Edison, A. S., Weinhold, F., and Markley, J. L. (1995) *J. Am. Chem. Soc. 117*, 9619−9624.
12. Loh, S. N., and Markley, J. L. (1994) *Biochemistry 33*, 1029−1036.
13. Bowers, P. M., and Klevit, R. E. (1996) *Nat. Struct. Biol. 3*, 522−531.
14. LiWang, A. C., and Bax, A. (1996) *J. Am. Chem. Soc. 118*, 12864−12865.
15. Kentsis, A., and Sosnick, T. R. (1998) *Biochemistry 37*, 14613−14622.
16. Khare, D., Alexander, P., and Orban, J. (1999) *Biochemistry 38*, 3918−3925.
17. Bowers, P. M., and Klevit, R. E. (2000) *J. Am. Chem. Soc. 122*, 1030−1033.
18. Krantz, B. A., Moran, L. B., Kentsis, A., and Sosnick, T. R. (2000) *Nature Struct. Biol. 7*, 62−71.
19. Hibbert, F., and Emsley, J. (1990) *Adv. Phys. Org. Chem. 26*, 255−379.
20. Harris, T. K., and Mildvan, A. S. (1999) *Proteins 35*, 275−282.
21. Shan, S. O., and Herschlag, D. (1996) *Proc. Natl. Acad. Sci. U.S.A. 93*, 14474−14479.
22. Huang, G. S., and Oas, T. G. (1995) *Biochemistry 34*, 3884−3892.
23. Burton, R. E., Huang, G. S., Daugherty, M. A., Calderone, T. L., and Oas, T. G. (1997) *Nat. Struct. Biol. 4*, 305−310.
24. Ghaemmaghami, S., Word, J. M., Burton, R. E., Richardson, J. S., and Oas, T. G. (1998) *Biochemistry 37*, 9179−9185.
25. Luo, P., and Baldwin, R. L. (1997) *Biochemistry 36*, 8413−8421.
26. Kreevoy, M. M., and Liang, T. M. (1980) *J. Am. Chem. Soc. 102*, 3315−3322.
27. Zhao, Q., Abeygunawardana, C., Talalay, P., and Mildvan, A. S. (1996) *Proc. Natl. Acad. Sci. U.S.A. 93*, 8220−8224.
28. Zhao, Q., Abeygunawardana, C., Gittis, A. G., and Mildvan, A. S. (1997) *Biochemistry 36*, 14616−14626.
29. Wu, Z. R., Ebrahimian, S., Zawrotny, M. E., Thornburg, L. D., Perez-Alvarado, G. C., Brothers, P., Pollack, R. M., and Summers, M. F. (1997) *Science 276*, 415−418.
30. Gerlt, J. A., Kreevoy, M. M., Cleland, W., and Frey, P. A. (1997) *Chem. Biol. 4*, 259−267.
31. Vishveshwara, S., Madhusudhan, M. S., and Maizel, J. V., Jr. (2001) *Biophys. Chem. 89*, 105−117.
32. Schowen, K. B., Limbach, H. H., Denisov, G. S., and Schowen, R. L. (2000) *Biochim. Biophys. Acta 1458*, 43−62.
33. Shan, S. O., Loh, S., and Herschlag, D. (1996) *Science 272*, 97−101.
34. Shan, S., and Herschlag, D. (1996) *J. Am. Chem. Soc. 118*, 5515−5518.
35. Perrin, C. L., and Nielson, J. B. (1997) *Annu. Rev. Phys. Chem. 48*, 511−544.
36. Cleland, W. W., and Kreevoy, M. M. (1994) *Science 264*, 1887−1890.
37. Frey, P. A., Whitt, S. A., and Tobin, J. B. (1994) *Science 264*, 1927−1930.
38. Frey, P. A. (1995) *Science 268*, 189.
39. Warshel, A., Papazyan, A., and Kollman, P. A. (1995) *Science 269*, 102−106.
40. Warshel, A., and Papazyan, A. (1996) *Proc. Natl. Acad. Sci. U.S.A. 93*, 13665−13670.
41. Warshel, A. (1998) *J. Biol. Chem. 273*, 27035−27038.
42. Warshel, A., and Papazyan, A. (1998) *Curr. Opin. Struct. Biol. 8*, 211−217.
43. Scheiner, S. (2000) *Biochim. Biophys. Acta 1458*, 28−42.
44. Ash, E. L., Sudmeier, J. L., De Fabo, E. C., and Bachovchin, W. W. (1997) *Science 278*, 1128−1132.
45. Kumar, G., and McAllister, M. (1998) *J. Org. Chem. 63*, 6968−6972.
46. Chen, J., McAllister, M., Lee, J., and Houk, K. (1998) *J. Org. Chem. 63*, 4611−4619.
47. Schah-Mohammedi, P., Shenderovich, I. G., Detering, C., Limbach, H.-H., Tolstoy, P. M., Smirnov, S. N., Denisov, G. S., and Golubev, N. S. (2000) *J. Am. Chem. Soc. 122*, 12878−12879.
48. Dunger, A., Limbach, H.-H., and Weisz, K. (2000) *J. Am. Chem. Soc. 122*, 10109−10114.
49. Buntkowsky, G., Sack, I., Limbach, H. H., Kling, B., and Fuhrhop, J. (1997) *J. Phys. Chem. B 101*, 11265−11272.
50. Benedict, H., Shenderovich, I. G., Malkina, O. L., Malkin, V. G., Denisov, G. S., Golubev, N. S., and Limbach, H.-H. (2000) *J. Am. Chem. Soc 122*, 1979−1988.
51. Ramos, M., Alkorta, I., Elguero, J., Golubev, N. S., Denisov, G. S., Benedict, H., and Limbach, H.-H. (1997) *J. Phys. Chem. A 101*, 9791−9800.
52. Branden, C., and Tooze, J. (1991) *Introduction to Protein Structure*, Garland Publishing, Inc., New York.
53. Bai, Y., Milne, J. S., Mayne, L., and Englander, S. W. (1993) *Proteins 17*, 75−86.
54. Wang, Y. L., and Gunn, J. R. (1999) *Can. J. Chem. 77*, 367−377.
55. Lowen, B., and Schulz, S. (1995) *Thermochim. Acta 262*, 69−82.
56. Mark, A. E., and van Gunsteren, W. F. (1994) *J. Mol. Biol. 240*, 167−176.
57. Brady, G. P., and Sharp, K. A. (1995) *J. Mol. Biol. 254*, 77−85.
58. Brady, G. P., Szabo, A., and Sharp, K. A. (1996) *J. Mol. Biol. 263*, 123−125.
59. D'Aquino, J. A., Gomez, J., Hilser, V. J., Lee, K. H., Amzel, L. M., and Freire, E. (1996) *Proteins 25*, 143−156.
60. Chakrabartty, A., Kortemme, T., and Baldwin, R. L. (1994) *Protein Sci. 3*, 843−852.
61. Avbelj, F., Luo, P., and Baldwin, R. L. (2000) *Proc. Natl. Acad. Sci. U.S.A. 97*, 10786−10791.
62. Scholtz, J. M., Marqusee, S., Baldwin, R. L., York, E. J., Stewart, J. M., Santoro, M., and Bolen, D. W. (1991) *Proc. Natl. Acad. Sci. U.S.A. 88*, 2854−2858.
63. Ross, P. D., and Rekharsky, M. V. (1996) *Biophys. J. 71*, 2144−2154.
64. Yang, A. S., and Honig, B. (1995) *J. Mol. Biol. 252*, 351−365.
65. Lazaridis, T., Archontis, G., and Karplus, M. (1995) *Adv. Protein Chem. 47*, 231−306.

BI011307T